

Machine Learning-Based Approach to Identify Inhibitors of Sterol-14-Alpha Demethylase: A Study on Chagas Disease

Jamiyu A Saliu, PhD

Department of Biochemistry, Adekunle Ajasin University, Akungba-Akoko, Nigeria.

Bioinformatics and Biology Insights
Volume 18: 1–9
© The Author(s) 2024
Article reuse guidelines:
sagepub.com/journals-permissions
DOI: 10.1177/11779322241262635



ABSTRACT

OBJECTIVES: Chagas Disease, caused by the parasite *Trypanosoma cruzi*, remains a significant public health concern, particularly in Latin America. The current standard treatment for Chagas Disease, benznidazole, is associated with various side effects, necessitating the search for alternative therapeutic options. In this study, we aimed to identify potential therapeutics for Chagas Disease through a comprehensive computational analysis.

METHODS: A library of compounds derived from *Cananga odorata* was screened using a combination of pharmacophore modeling, structure-based screening, and quantitative structure-activity relationship (QSAR) analysis. The pharmacophore model facilitated the efficient screening of the compound library, while the structure-based screening identified hit compounds with promising inhibitory potential against the target enzyme, sterol-14-alpha demethylase.

RESULTS: The QSAR model predicted the bioactivity of the hit compounds, revealing one compound to exhibit superior activity compared to benznidazole. Evaluation of the physicochemical, pharmacokinetic, toxicity, and medicinal chemistry properties of the hit compounds indicated their drug-like characteristics, oral bioavailability, ease of synthesis, and reduced toxicity profiles.

CONCLUSION: Overall, our findings present a promising avenue for the discovery of novel therapeutics for Chagas Disease. The identified hit compounds possess favorable drug-like properties and demonstrate potent inhibitory effects against the target enzyme. Further in vitro and in vivo studies are warranted to validate their efficacy and safety profiles.

KEYWORDS: Chagas, pharmacophore, quantitative structure-activity relationship, *Cananga odorata*, in silico

RECEIVED: June 5, 2023. **ACCEPTED:** May 23, 2024.

TYPE: Original Research Article

FUNDING: The author(s) received no financial support for the research, authorship, and/or publication of this article.

DECLARATION OF CONFLICTING INTERESTS: The author(s) declared no potential conflicts of interest with respect to the research, authorship, and/or publication of this article.

CORRESPONDING AUTHOR: Jamiyu A Saliu, Department of Biochemistry, Adekunle Ajasin University, Akungba-Akoko 342111, Nigeria. Email: jamiyu.saliu@aau.edu.ng

Introduction

Chagas Disease (CD), also known as the American trypanosomiasis, is a neglected tropical disease recognized by the World Health Organization. It is characterized by symptoms such as swelling at the site of infection and fever, and if left untreated, it can lead to congestive heart failure. The disease is caused by exposure to the feces of the triatomine bug, a vector that carries the parasite *Trypanosoma cruzi*. The name “Kissing Bug” originates from the bug’s tendency to bite people’s faces during feeding. Chagas Disease is endemic to Latin American countries, spanning from Southern United States to Mexico and Argentina.¹ The triatomine bug thrives in poor housing conditions, putting individuals in rural areas at a higher risk of infection. While vector-borne transmission has historically been the primary mode of infection, CD can also be transmitted through blood transfusion and from mother to child during pregnancy.²

In recent years, significant progress has been made in reducing the transmission of *T. cruzi* through extensive vector control and donor screening programs implemented in many endemic countries. However, several barriers continue to hinder the effective management of the disease. These barriers include challenges related to healthcare financing and payment,

limitations in screening and diagnosis methods, suboptimal effectiveness of available treatments, and insufficient awareness among healthcare providers, as well as the general public regarding CD.^{2,3} Benznidazole and nifurtimox are Food and Drug Administration-approved drugs commonly used to treat CD. However, both drugs have their limitations. Benznidazole, for instance, exhibits a mechanism of action that involves the preferential oxidation of the nucleotide pool, resulting in the incorporation of oxidized nucleotides during DNA replication. This process leads to the formation of potentially lethal double-stranded DNA breaks in the DNA of *T. cruzi*, the parasite causing CD.⁴ Despite its effectiveness, benznidazole has certain drawbacks. It is primarily prescribed for children aged 2 to 12 years and has been associated with side effects such as infertility in men and potential harm to unborn babies.⁵ In addition, individuals taking benznidazole may experience severe skin reactions, including sore throat, fever, and skin rash.⁶ These factors highlight the need for alternative treatment options that can reduce the occurrence of such side effects.

Sterol-14-demethylase is a crucial enzyme belonging to the heme-containing cytochrome P450 family, and it plays a significant role in the synthesis of sterols in eukaryotes.^{7,8} In protozoa like *T. cruzi*, ergosterol is synthesized as the final product



of sterol biosynthesis, contrasting with the production of cholesterol in mammals. The synthesis of ergosterol involves the elimination of the 14 α -methyl group from sterol precursors, a process catalyzed by sterol-14-demethylase.⁹ In Trypanosomatidae, a family of parasites that includes *T. cruzi*, the causative agent of CD, the synthesis of endogenous sterols is of utmost importance. These sterols not only serve as structural components of the parasites' membranes but also function as hormonal molecules that regulate various cellular processes, including cell development, multiplication, and morphological transformation, at remarkably low concentrations.¹⁰

While *T. cruzi* can incorporate sterols, primarily cholesterol, from its mammalian host into its membranes, it also relies on de novo sterol synthesis for its survival in all stages of its life cycle. Consequently, the parasite is highly vulnerable to sterol biosynthesis inhibitors.⁹ Inhibiting sterol-14-demethylase, the enzyme responsible for a critical step in sterol biosynthesis, has been explored as a potential therapeutic approach against *T. cruzi* and other related parasites.^{11–13} By targeting this enzyme, it is possible to disrupt the synthesis of essential sterols, which can ultimately lead to the inhibition of parasite growth and survival.

The utilization of plant-derived inhibitors holds great promise in terms of their suitability for oral administration, affordability, and accessibility. One such plant of interest is *Cananga odorata*, commonly known as “ylang-ylang,” which has a rich history as a traditional medicinal plant in South-Eastern Asian countries like the Philippines and Malaysia.¹⁴ *C. odorata* is a medium-sized tree that can reach heights of up to 15 m. Extensive research has highlighted the diverse therapeutic properties of *C. odorata*. It has been recognized for its antimicrobial, antibiofilm, antioxidant, insecticidal, anti-inflammatory, and antibacterial effects.^{14,15} In a study, three compounds extracted from *C. odorata*, namely O-methylmoschatoline, liri-odenine, and 3,4-dihydroxybenzoic acid, exhibited notable antibacterial and antifungal activities.¹⁶ Furthermore, another constituent from *C. odorata*, N-trans-feruloyltyramine, identified in the methanolic extract of the seeds, was found to potentially contribute to the suppression of melanogenesis by inhibiting the expression of the tyrosinase enzyme.¹⁷

These bioactive properties make *C. odorata* a valuable resource for potential drug discovery and development. By harnessing the beneficial compounds present in *C. odorata*, it may be possible to develop novel oral treatments that are cost effective and readily available.

This study utilized computational techniques to identify potential inhibitors of sterol-14-demethylase from *C. odorata*. The objective was to find phytoconstituents with anti-trypanosomal activity. The workflow included structure-based screening, molecular docking, quantitative structure-activity relationship (QSAR) analysis, pharmacophore modeling, and pharmacokinetic assessments. The findings could contribute to the development of novel drugs for treating trypanosomal infections using compounds from *C. odorata*.

Materials and Method

Protein selection and preparation

The sterol-14-alpha demethylase enzyme, with a Protein Data Bank (PDB) ID of 4CKA, was obtained from the official website of the PDB (<https://www.rcsb.org/>). Before its use in this study, the protein underwent thorough preprocessing and was subjected to modifications aimed at optimizing the assignment of hydrogen bonds and minimizing its structure using the OPLS3e force field.¹⁸ The resulting minimized protein was then utilized for further analyses and investigations.

Ligand generation and preparation

A compound library for *C. odorata* was generated in SDF format by retrieving relevant compounds from the PubChem web database (Supplemental Table 1). The retrieved compounds underwent further processing using the LigPrep tool. This tool facilitated the conversion of the initially available two-dimensional molecules into three-dimensional structures. The process involved ionizing the molecules at a pH of 7.2 ± 0.2 and eliminating any salts present using Epik. The OPLS3 force field was applied to ensure accurate ionization and tautomeric state representation of the compounds.¹⁹

Receptor grid generation

To identify the specific region of interaction between the ligand and protein, a receptor grid was created. This grid, known as the Glide Grid, was constructed using the Receptor Grid Generation tool and focused on the binding domain of the protein.²⁰ By selecting the co-crystallized ligand situated at the active site of 4CKA, the binding location was determined. To facilitate the subsequent process of molecular docking, a grid box was automatically generated for the protein. The dimensions of the grid box were defined as follows: $X=0.86$, $Y=27.49$, and $Z=456.75$.

Pharmacophore modeling and screening

The receptor-ligand complex was extensively studied, and a hypothesis (E-pharmacophore) was generated using the phase interface within the Schrödinger suite. This pharmacophore was designed to highlight the key properties that play a crucial role in the specific binding of the ligand to the active sites of the target protein.²¹ Subsequently, the hypothesis was employed as a filtering criterion to eliminate compounds that did not exhibit at least two out of the five essential features identified by the pharmacophore analysis.

Molecular docking

The molecular docking process was performed using the Glide tool, utilizing Maestro 11.1 software. The compound library, which had already been filtered down to 28 compounds, was

docked into the prepared grid of protein targets. Two docking algorithms were employed: Standard Precision (SP) and the more rigorous Extra Precision (XP) algorithms. Initially, compounds with a docking score of less than -5.0 kcal/mol using the SP algorithm were filtered out, resulting in the exclusion of four compounds. The remaining selected compounds (24) were then subjected to XP docking. During the docking process, the protein was considered a rigid body, while the ligand's rotatable bonds were allowed to freely move and adopt different conformations.²²

Molecular mechanics generalized born surface area

Molecular mechanics-generalized Born surface area (MM-GBSA) is a computational method used to calculate the energy of various components involved in a molecular system, including optimized free receptors, free ligands, and the complex formed by the ligand binding to the receptor. In addition, it enables the evaluation of ligand strain energy by placing the ligand in a solvent environment generated by the VSGB 2.0 suite. In this study, Prime rotamer search techniques available in Maestro were employed in conjunction with the OPLS3 force field and the VSGB solvent model. These tools and models were utilized to perform the necessary calculations and simulations. The binding free energy, which quantifies the strength of the interaction between the ligand and receptor, was determined using the following equation:

$$\Delta G^{\text{bind}} = G^{\text{complex}} - (G^{\text{protein}} + G^{\text{Ligand}}) \quad (1)$$

This equation takes into account various energy contributions from the molecular system and provides valuable insights into the binding affinity between the ligand and receptor.²¹

Development of AutoQSAR Model

To gather information about sterol-14- α demethylase inhibitors' activity, a total of 38 inhibitors were retrieved from the ChEMBL database. The protein's FASTA sequence, obtained from the PDB, was used as a query to extract these compounds. To facilitate further analysis, the extracted compounds were converted into the ".SDF" file format using Data Warrior software.¹⁸ Using the AutoQSAR module, a QSAR model was constructed utilizing these compounds. Multiple models were generated, and among them, the kpls_radial_44 model was identified as the best-performing model based on its rank and predictive capability. Subsequently, this selected model, kpls_radial_44, was employed to predict the pIC₅₀ values of the top-ranked compounds as well as a standard compound. This QSAR model allowed for the estimation of the inhibitory activity of these compounds, providing valuable insights into their potential as sterol-14- α demethylase inhibitors.

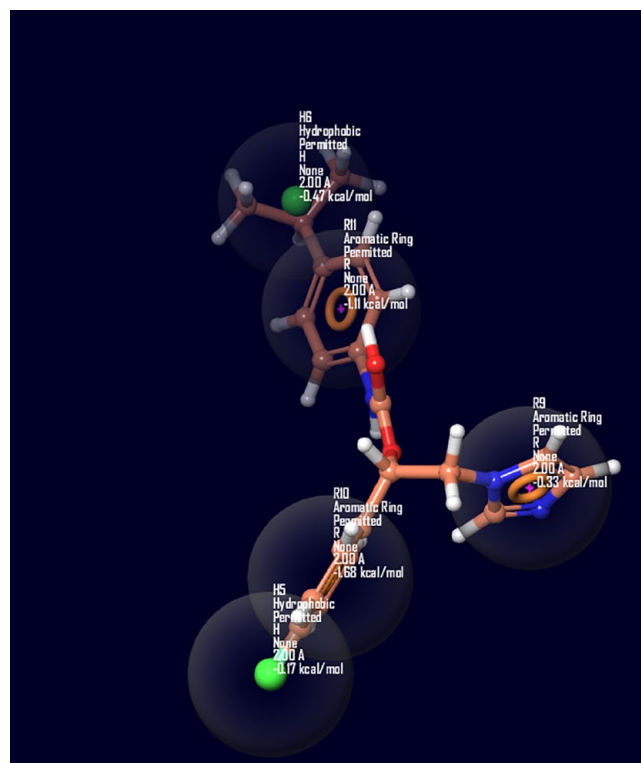


Figure 1. Pharmacophore hypothesis generated.

Absorption Distribution Metabolism Excretion/Toxicity screening

To assess the absorption, distribution, metabolism, and excretion (ADME) characteristics of the top five compounds, as well as the standard drug, their efficacy was predicted using the admetSAR server. The admetSAR server (<http://lmmd.ecust.edu.cn/admetSar2/>) provides valuable predictions regarding the ADME properties of compounds. These properties play a vital role in drug development as they help evaluate the potential of a compound to become an effective drug. By analyzing these characteristics, valuable insights can be gained regarding the compound's ADME, contributing to the decision-making process in drug discovery and development.²²

Result and Discussion

Before molecular docking, a pharmacophore hypothesis was developed based on the complex formed by the protein and co-crystallized ligand. The PHASE module in Schrödinger suite was employed to extract essential information regarding the molecular orientation of crucial functional groups involved in the high-affinity binding of ligands to the protein target.

The resulting E-pharmacophore hypothesis (Figure 1) consisted of two hydrophobic groups and three aromatic rings. The pharmacophore hypothesis was used to filter the library of

Table 1. Docking scores of the top-scoring compounds and standard against sterol-14-alpha demethylase.

PUBCHEM ID	COMPOUND NAME	DOCKING SCORES	MM-GBSA
8363	Benzyl salicylate	-7.627	-43.729
518975	Calamenene	-7.453	-30.424
2345	Benzyl benzoate	-6.305	-38.262
15118	5-Indanol	-6.151	-31.948
7463	p-Cymene	-6.048	-31.003
31593	Benznidazole (reference drug)	-6.817	-41.157

Abbreviation: MM-GBSA, molecular mechanics-generalized Born surface area.

compounds, allowing for the identification of ligands that possess similar key features important for binding to the target protein.

The molecular docking analysis identified five compounds from *C odorata* that demonstrated strong inhibitory potential against the target enzyme, with docking scores comparable to the standard compound benznidazole (Supplemental Figure 1). A more negative docking score indicates a higher inhibitory potential. The compounds benzyl salicylate, calamenene, benzyl benzoate, 5-indanol, and p-cymene exhibited excellent inhibitory potential, with docking scores of -7.627, -7.453, -6.305, -6.151, and -6.058 kcal/mol, respectively, compared to the docking score of -6.817 kcal/mol for benznidazole, which is a standard drug used to treat CD (Table 1).

Structural-based drug design focuses primarily on the interaction between the protein and ligand, as the extent of inhibition is largely determined by the ligand's interaction with specific amino acid residues at the active site of the target enzyme.²³ Table 2 and Figure 2 present the key interactions contributing significantly to the inhibition of

sterol-14-demethylase in this study. Benzyl salicylate formed a single hydrogen bond with LYS 421, while calamenene formed a single PI-PI stacking bond with TYR 103. Benzyl benzoate also formed a single PI-PI stacking bond with PHE 290. 5-Indanol made a single H-bond interaction with ALA 287. Benznidazole, the standard, made two H-bonds with TYR 116.

In addition, the MM-GBSA technique provides a more accurate estimation of the binding free energies (dG) for protein-ligand complexes. Negative values indicate stable complexes in the target's binding pocket. In this study, all lead compounds exhibit negative values, indicating their stability within the target's binding pocket. The binding free energies for the docked complexes were -43.729, -30.424, -38.262, -31.948, and -31.003 kcal/mol for benzyl salicylate, calamenene, benzyl benzoate, 5-indanol, and p-cymene, respectively. This suggests that all the hit compounds are more stable in the target's binding pocket. Benznidazole, the standard, exhibits a binding free energy of -41.157 kcal/mol. The utilization of the MM-GBSA technique enhances the accuracy of virtual screening results and provides valuable insights into the stability of protein-ligand complexes within the binding pocket. The negative binding free energy values obtained for the lead compounds indicate their favorable binding characteristics, further supporting their potential as effective inhibitors.

AutoQSAR

Quantitative structure-activity relationship analysis is a crucial computational tool in drug discovery that explores the relationship between the structural characteristics of small molecules and their biological activities.²⁴

In this study, the AutoQSAR module within the Schrodinger suite was employed, utilizing various topological descriptors to construct independent variable models based on experimental data generated for the target.

Table 2. Interaction profile of top-ranked compounds including the standard within the active site of sterol-14-alpha demethylase.

COMPOUND NAME	H-BOND	HYDROPHOBIC AMINO ACID	OTHER INTERACTIONS
Benzyl salicylate	LYS 421	MET 284, ALA 287, MET 123, VAL 114, ALA 115, TYR 116, LEU 127, LEU 130, ALA 291, ILE 423, CYS 422	None
Calamenene	None	MET 460, MET 106, ILE 105, TYR 103, VAL 102, VAL 213, PHE 290, PHE 110, LEU 356, MET 358, VAL 359, MET 360	PI-PI stacking: TYR 103
Benzyl benzoate	None	TYR 116, PHE 110, ALA 291, PHE 290, LEU 208, MET 106, ILE 105, TYR 103, VAL 102, VAL 213, MET 360, VAL 359, MET 358, LEU 356, MET 460, VAL 461	PI-PI stacking: PHE 290
5-Indanol	ALA 287	MET 123, LEU 127, VAL 114, ALA 115, TYR 116, LEU 130, MET 284, ALA 287, ALA 288, ALA 291, ILE 423	None
p-Cymene	None	TYR 116, PHE 110, VAL 102, TYR 103, ILE 105, MET 106, VAL 213, MET 460, ALA 291, PHE 290	PI-PI stacking: TYR 103
Benznidazole	TYR 116	PHE 110, ALA 115, TYR 116, MET 123, LEU 127, LEU 130, MET 284, ALA 287, ALA 288, ILE 423, CYS 422	None

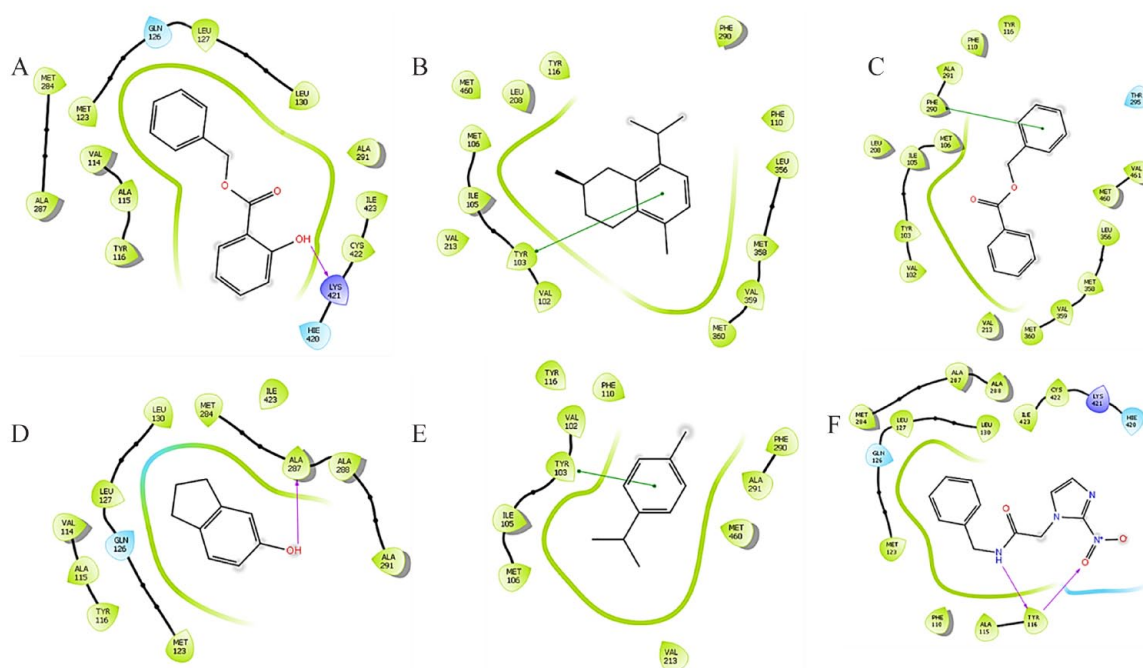


Figure 2. Two-dimensional interaction of the hits and the standard. Benznidazole in the active site of the enzyme. (A) Benzyl salicylate, (B) calamenene, (C) benzyl benzoate, (D) 5-indanol, (E) p-cymene, (F) benznidazole (standard).

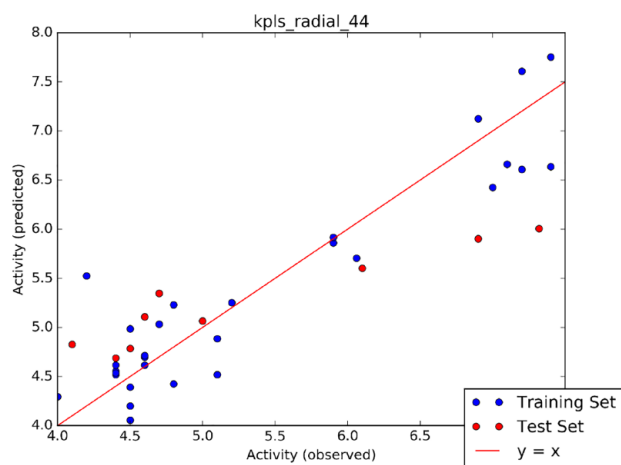


Figure 3. Scatter plot for the best AutoQSAR model (kpls_radial_44).

Among the generated QSAR models, the kpls_radial_44 model (Figure 3) emerged as the best-performing model, trained using machine learning techniques. The model's performance was evaluated using key parameters such as SD (0.4412), coefficient of determination (0.8581), root mean squared error (0.695), and cross-validation (0.6087; Table 3). Table 4 shows the test and training set utilized in generating the model.

Subsequently, the QSAR model was employed to predict the pIC₅₀ values of the hit compounds listed in Table 5. The

Table 3. Parameters of the QSAR model.

SD	R ²	RMSE	Q ²
0.4412	0.8581	0.695	0.6087

Abbreviations: QSAR, quantitative structure-activity relationship; RMSE, root mean squared error.

obtained pIC₅₀ values for the hit compounds are also presented in Table 5. Notably, only benzyl benzoate demonstrated a superior pIC₅₀ value (5.349 nM) compared to the standard drug (5.331 nM).

ADMET and Drug Likeness

The analysis of ADME is a crucial aspect of the drug discovery process, providing valuable insights into the behavior of drugs within a biological system.²⁵ In this study, we employed the admetSAR server to predict the drug-like properties and potential toxicity of the selected lead compounds and the standard compound.

To evaluate the drug likeness of the compounds, we employed the Lipinski rule, which encompasses five key criteria for determining oral activity.²⁶ The results, presented in Table 6, demonstrate that all of the selected compounds exhibit favorable physicochemical properties, including low molecular weight, a desirable bioavailability score, and good solubility. Notably, these properties position the lead compounds as top

Table 4. Train and test set for the QSAR model.

ID	MOLECULE CHEMBL ID	SET	Y(OBSERVED)	Y(PREDICTED)	ERROR
1	CHEMBL106	Train	6.06	5.7052	-0.3548
2	CHEMBL1397	Test	7.32	6.0042	-1.3158
3	CHEMBL3431444	Train	4.4	4.5544	0.1544
4	CHEMBL4208391	Train	7	6.4239	-0.5761
5	CHEMBL3431178	Test	4.6	5.1088	0.5088
6	CHEMBL3431173	Train	4.8	4.4249	-0.3751
7	CHEMBL1731664	Train	4.5	4.2013	-0.2987
8	CHEMBL3431374	Train	6.9	7.1254	0.2254
9	CHEMBL3430913	Train	4.4	4.5206	0.1206
10	CHEMBL1535535	Train	7.4	7.7529	0.3529
11	CHEMBL3431283	Train	4	4.2952	0.2952
12	CHEMBL3431128	Train	4.6	4.6983	0.0983
13	CHEMBL3431361	Train	5.1	4.5195	-0.5805
14	CHEMBL3431357	Train	4.8	5.2313	0.4313
15	CHEMBL3431261	Train	7.2	7.607	0.407
16	CHEMBL3431334	Test	4.5	4.7851	0.2851
17	CHEMBL3431264	Test	6.1	5.6039	-0.4961
18	CHEMBL3431263	Train	7.2	6.6093	-0.5907
19	CHEMBL3430988	Train	4.6	4.6178	0.0178
20	CHEMBL3431347	Train	4.4	4.5353	0.1353
21	CHEMBL530358	Train	5.2	5.2533	0.0533
22	CHEMBL3431331	Test	6.9	5.9036	-0.9964
23	CHEMBL2165401	Test	4.1	4.829	0.729
24	CHEMBL3430943	Train	4.6	4.7152	0.1152
25	CHEMBL3430944	Train	4.4	4.6171	0.2171
26	CHEMBL3431341	Train	5.1	4.8857	-0.2143
27	CHEMBL3431358	Train	5.9	5.8619	-0.0381
28	CHEMBL3430976	Train	4.2	5.5247	1.3247
29	CHEMBL3431279	Test	4.4	4.6889	0.2889
30	CHEMBL3430915	Train	7.1	6.6605	-0.4395
31	CHEMBL3431387	Train	4.5	4.3918	-0.1082
32	CHEMBL3431309	Train	4.5	4.055	-0.445
33	CHEMBL3431021	Train	5.9	5.9178	0.0178
34	CHEMBL3431177	Train	4.7	5.0342	0.3342
35	CHEMBL3431020	Train	7.4	6.6348	-0.7652
36	CHEMBL3431101	Train	4.5	4.9855	0.4855
37	CHEMBL3431119	Test	5	5.0655	0.0655
38	CHEMBL3431410	Test	4.7	5.3462	0.6462

Abbreviation: QSAR, quantitative structure-activity relationship.

Table 5. Predicted pIC50 values of hit compounds and standard.

PUBCHEM ID	COMPOUND NAME	PREDICTED PIC50
8363	Benzyl salicylate	5.264
518975	Calamenene	4.940
2345	Benzyl benzoate	5.349
15118	5-Indanol	4.873
7463	p-Cymene	4.890
31593	Benznidazole (reference drug)	5.331

drug-like candidates based on their physicochemical profiles. In addition, none of the compounds violated more than one of the Lipinski rule criteria. The implicit log P (iLogP) value is utilized to measure the n-octanol/water partition coefficient of compounds, measuring their lipophilicity. Lipophilicity impacts a drug's solubility and permeability across membranes, with iLogP being a predictive method used for this purpose.²⁷ All compounds, including the standard, were predicted to exhibit lipophilic characteristics, as their values were below five. Veber's rule says that compounds with a polar surface area (TPSA) <140 Å² tend to have favorable oral bioavailability. In this case, all compounds displayed TPSA scores below 140. The logKp values, measured in cm/s, for the compounds, including the standard, were predicted to range from -3.96 to -7.24. A more negative logKp value suggests a lower ability for the molecule to pass through the skin.²⁸ Benznidazole, the standard drug, was predicted to have the lowest skin permeability score (-7.24 cm/s).

In terms of blood-brain barrier (BBB) permeability, all test compounds, except benzyl salicylate, were predicted to cross the BBB. The BBB serves as a crucial barrier that regulates the entry of molecules into the central nervous system from the bloodstream, controlling access to the brain.²⁹ P-glycoprotein (P-gp), a transmembrane efflux pump, plays a role in expelling drugs out of cells, which can potentially lead to poor drug efficacy or therapeutic failure.³⁰ However, the results indicate that the hit compounds, including the standard, are non-substrates and

non-inhibitors of P-gp. This suggests that these compounds are less likely to be affected by P-gp-mediated efflux and may exhibit improved drug effectiveness.

The cytochrome P450 (CYP450) enzymes are responsible for metabolizing therapeutic drugs and play a crucial role in drug clearance within the liver.³¹ Inhibition of CYP450 isoforms can lead to drug-drug interactions and impact drug toxicity profiles. In our assessment, we found that none of the hit compounds, including the standard, were predicted to be substrates or inhibitors of CYP3A4, a commonly studied CYP450 isoform. Similar results were observed for the CYP2C9 isoform, indicating a lower likelihood of drug interactions mediated by these enzymes. Furthermore, none of the compounds were predicted to inhibit CYP2D6 (Figure 4).

Toxicity analysis revealed that all compounds, including the standard drug, demonstrated non-carcinogenic and non-eye corrosive properties. However, it is important to note that only the standard drug was predicted to have mutagenic potential based on the results of the Ames mutagenesis test, which assesses the likelihood of a chemical causing mutagenic or carcinogenic effects.³²

Various studies have explored the inhibition of sterol-14-demethylase through different approaches. Kulactone and galocatechin emerged as potent inhibitors in an *in silico* study, as determined by extensive molecular dynamics simulations.²² Alternatively, a study focused on synthesizing potential antimicrobial compounds, specifically 1,3-phenylene-based symmetrical bis(urea-1,2,3-triazole) hybrids, demonstrated inhibitory effects on the sterol-14-demethylase enzyme. Benzyl salicylate, identified as a hit compound in this study, demonstrated anti-inflammatory activity by inhibiting the expression of inducible nitric oxide synthase and cyclooxygenase-2.³³ In addition, calamenene (also identified as a hit compound in this study) and its analogs, Cala 1 and Cala 2, reported in another study, exhibited antibacterial properties.³⁴

Conclusion

In conclusion, this study focused on identifying potential therapeutics for CD through a comparative analysis with the

Table 6. Drug likeness prediction of the hit compounds and standard.

ENTRY NAME	MW	HBA	HBD	ILOGP	PSA	LOGKP	ROV
Benzyl salicylate	228.24	3	1	2.63	46.53	-5.43	0
Calamenene	202.34	0	0	3.24	0.0	-3.96	1
Benzyl benzoate	212.24	2	0	2.68	26.30	-4.78	0
5-Indanol	134.18	1	1	1.80	20.23	-5.44	0
p-Cymene	134.22	0	0	2.51	0.00	-4.21	1
Benznidazole (reference drug)	260.25	4	1	1.15	92.74	-7.24	0

Abbreviations: iLogP, implicit log P; PSA, polar surface area; MW, Molecular weight; HBA, number of Hydrogen bond acceptor; HBD, number of Hydrogen bond donor; ROV, rule of five (Lipinski's).

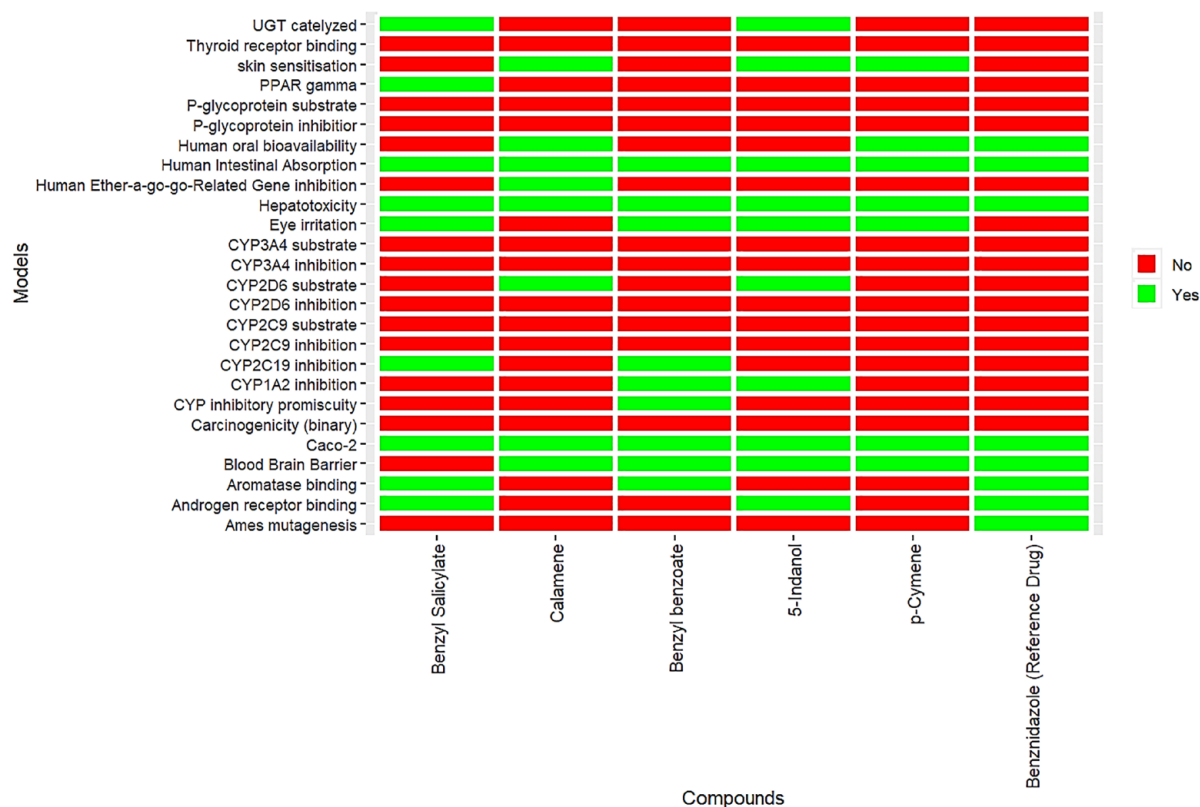


Figure 4. ADMET properties of the hit compounds and standard.

Abbreviations: ADMET, Absorption Distribution Metabolism Excretion and Toxicity; UGT, Uridine Diphosphate-Glucuronosyltransferase; PPAR, Peroxisome proliferator-activated receptor; CYP, Cytochrome p450; Caco, Cancer coli.

standard drug, benznidazole. I employed a computational approach, utilizing various tools and models to screen a library of compounds derived from *C. odorata*. Through pharmacophore modeling and structure-based screening, I successfully identified several hit compounds that showed promising bioactivity against the target enzyme, sterol-14- α demethylase. In addition, the QSAR model predicted one of the hits to exhibit superior bioactivity compared to benznidazole. Furthermore, I conducted a comprehensive evaluation of the physicochemical, pharmacokinetic, toxicity, and medicinal chemistry properties of the identified lead compounds. The results indicated that these compounds possess drug-like characteristics, are orally bioavailable, are easily synthesizable, and exhibit reduced toxicity profiles, making them potential candidates for further development.

While these findings provide valuable insights and initial evidence of the efficacy of these compounds, further in vitro and in vivo studies are necessary to confirm their therapeutic potential. Continued research and evaluation of these compounds will contribute to the development of alternative and safer treatments for CD, addressing the limitations associated with the current standard therapy.

Acknowledgements

None

Author Contributions

Jamiyu A Saliu performed the study and wrote the manuscript.

Ethical Statement

Not applicable

SUPPLEMENTAL MATERIAL

Supplemental material for this article is available online.

REFERENCES

- Pérez-Molina JA, Molina I. Chagas disease. *Lancet*. 2018;391:82-94. doi:10.1016/S0140-6736(17)31612-4
- Kirchhoff LV. Epidemiology of American trypanosomiasis (Chagas disease). *Adv Parasitol*. 2011;75:1-18.
- Mills RM. Chagas disease: epidemiology and barriers to treatment. *Am J Med*. 2020;133:1262-1265.
- Rajão MA, Furtado C, Alves CL, et al. Unveiling benznidazole's mechanism of action through overexpression of DNA repair proteins in *Trypanosoma cruzi*. *Environ Mol Mutagen*. 2014;55:309-321.
- Pinazo MJ, Muñoz J, Posada E, et al. Tolerance of benznidazole in treatment of Chagas' disease in adults. *Antimicrob Agents Chemother*. 2010;54:4896-4899.
- Viotti R, Vigliano C, Lococo B, et al. Side effects of benznidazole as treatment in chronic Chagas disease: fears and realities. *Expert Rev Anti Infect Ther*. 2009;7:157-163.
- Zarn JA, Brüscheiler BJ, Schlatter JR. Azole fungicides affect mammalian steroidogenesis by inhibiting sterol 14 α -demethylase and aromatase. *Environ Health Perspect*. 2003;111:255-261.
- Lepesheva GI, Waterman MR. Sterol 14 α -demethylase cytochrome P450 (CYP51), a P450 in all biological kingdoms. *Biochim Biophys Acta*. 2007;1770:467. doi:10.1016/j.bbagen.2006.07.018

9. Buckner FS, Urbina JA. Recent developments in sterol 14 α -demethylase inhibitors for Chagas disease. *Int J Parasitol Drugs Drug Resist.* 2012;2:236-242. doi:10.1016/j.ijpddr.2011.12.002
10. Friggeri L, Hargrove TY, Rachakonda G, et al. Sterol 14 α -demethylase structure-based optimization of drug candidates for human infections with the protozoan Trypanosomatidae. *J Med Chem.* 2018;61:10910-10921.
11. Matin MM, Chakraborty P, Alam MS, Islam MM, Hance U. Novel mannopyranoside esters as sterol 14 α -demethylase inhibitors: synthesis, PASS prediction, molecular docking, and pharmacokinetic studies. *Carbohydr Res.* 2020;496:108130.
12. Lone SA, Khan S, Ahmad A. Inhibition of ergosterol synthesis in *Candida albicans* by novel eugenol tosylate congeners targeting sterol 14 α -demethylase (CYP51) enzyme. *Arch Microbiol.* 2020;202:711-726.
13. Geesi MH, Riadi Y, Kaiba A, et al. Synthesis, antimicrobial evaluation, crystal structure, Hirshfeld surface analysis and docking studies of 4-[2-(1-methyl-1H-imidazol-2-ylsulfanyl)-acetyl-amino]-benzenesulfonic acid. *J Mol Struct.* 2022;1265:133425.
14. Tan LTH, Lee LH, Yin WF, et al. Traditional uses, phytochemistry, and bioactivities of *Cananga odorata* (Ylang-ylang). *Evid Based Complement Alternat Med.* 2015;2015:896314.
15. Harahap D, Niaci S, Mardina V, et al. Antibacterial activities of seven ethnomedicinal plants from family Annonaceae. *J Adv Pharm Technol Res.* 2022;13:148-153.
16. Chao S, Young G, Oberg C, Nakaoka K. Inhibition of methicillin-resistant *Staphylococcus aureus* (MRSA) by essential oils. *Flav Frag J.* 2008;23:444-449.
17. Efdi M, Ohguchi K, Akao Y, Nozawa Y, Koketsu M, Ishihara H. N-transferuloyltyramine as a melanin biosynthesis inhibitor. *Biol Pharm Bull.* 2007;30:1972-1974.
18. Bodun DS, Omoboyowa DA, Adedara JF, et al. Virtual screening of flavonoids from *Blighia sapida* against ERK5 involved in breast cancer. *Proc Indian Natl Sci Acad.* 2023;89:957-966.
19. Olugbogi EA, Bodun DS, Omooseye SD, et al. *Quassia amara* bioactive compounds as a Novel DPP-IV inhibitor: an in-silico study. *Bull Natl Res Centre.* 2022;46:1-14.
20. Omoboyowa DA, Bodun DS, Saliu JA. Structure-based in silico investigation of antagonists of human ribonucleotide reductase from *Annona muricata*. *Inform Med Unlock.* 2023;38:101225.
21. Bodun DS, Omoboyowa DA, Omotuyi OI, et al. QSAR-based virtual screening of traditional Chinese medicine for the identification of mitotic kinesin Eg5 inhibitors. *Comput Biol Chem.* 2023;104:107865.
22. Omoboyowa DA, Kareem JA, Saibu OA, Bodun DS, Ajayi TM, Oyenyin OE. Identification of phyto-compounds from *Ilex kudingcha* as inhibitors of sterol-14 α -demethylase protease: a computational approach against Chagas disease. *Chem Africa.* 2023;6:1335-1347.
23. Zhang S, Krumberger M, Morris MA, Parrocha CMT, Kreutzer AG, Nowick JS. Structure-based drug design of an inhibitor of the SARS-CoV-2 (COVID-19) main protease using free software: a tutorial for students and scientists. *Euro J Med Chem.* 2021;218:113390.
24. De P, Kar S, Ambure P, Roy K. Prediction reliability of QSAR models: an overview of various validation tools. *Arch Toxicol.* 2022;96:1279-1295.
25. Kar S, Leszczynski J. Open access in silico tools to predict the ADMET profiling of drug candidates. *Expert Opin Drug Discov.* 2020;15:1473-1487.
26. Lipinski CA. Lead-and drug-like compounds: the rule-of-five revolution. *Drug Discov Today Technol.* 2004;1:337-341.
27. Zadorozhnyi PV, Kiselev VV, Kharchenko AV. In silico toxicity evaluation of Salubrinal its analogues. *Eur J Pharm Sci* 2020;155:105538.
28. Rudrappa M, Nayaka S, Kumar RS. In silico molecular docking approach of melanin against melanoma causing MITF proteins and anticancer, oxidation-reduction, photoprotection, and drug-binding affinity properties of extracted melanin from *Streptomyces* sp. strain MR28. *Appl Biochem Biotechnol.* 2023;195:4368-4386.
29. Profaci CP, Munji RN, Pulido RS, Daneman R. The blood-brain barrier in health and disease: important unanswered questions. *J Exp Med.* 2020;217:e20190062.
30. Dong J, Qin Z, Zhang WD, et al. Medicinal chemistry strategies to discover P-glycoprotein inhibitors: an update. *Drug Resist Updat.* 2020;49:100681.
31. Klomp SD, Manson ML, Guchelaar HJ, Swen JJ. Phenoconversion of cytochrome P450 metabolism: a systematic review. *J Clin Med.* 2020;9:2890.
32. Zeiger E. The test that changed the world: the Ames test and the regulation of chemicals. *Mutat Res Genet Toxicol Environ Mutagen.* 2019;841:43-48.
33. Lee D, Alishir A, Jang TS, Kim KH. Identification of bioactive natural product from the stems and stem barks of *Cornus walteri*: benzyl salicylate shows potential anti-inflammatory activity in lipopolysaccharide-stimulated RAW 264.7 macrophages. *Pharmaceutics.* 2021;13:443.
34. Limna Mol VP, Abdulaziz A, Sneha KG, Praveen PJ, Raveendran TV, Parameswaran PS. Inhibition of pathogenic *Vibrio parvulus* using calamenene, derived from the Indian gorgonian *Subergorgia reticulata*, and its synthetic analog. *J Biotech.* 2020;10:248-247.